Adsorption (2006) 12:375–392
DOI 10.1007/s10450-006-0566-9

Simulated moving bed technology: old and new

Pedro Sá Gomes · Mirjana Minceva ·
Alírio E. Rodrigues

Abstract The Simulated Moving Bed (SMB) concept has been applied to the separation of different mixtures as a continuous counter current separation process, avoiding several problems related with solid motion. The aim of this work is to present some relevant examples of SMB separations corresponding to the two major ages in the use of the SMB concept, here named "old" and "new" applications. The "old" applications of SMB technology in the petrochemical industry are still important, with large and highly productive units; and the "new" applications of the second "age" of SMB concept are from the fine chemical, pharmaceutical and biochemistry areas, associated with the demand of high purity products during the last 10 years.

Different examples are presented for different ages: a UOP Parex® process for the "old", modelled with the equivalent True Moving Bed (TMB) approach; and a chiral resolution for the "new", modelled by the real SMB model. Some of the latest developments are also mentioned: the non conventional techniques as the Varicol® process, PowerFeed, Modicon, M3C or Enriched Extract-SMB (EE-SMB), MultiFeed (MF), Outlet Streams Swing (OSS) or Pseudo-SMB, involving considerable changes in the SMB concept itself. The use of the last optimization/modelling packages for the development of design techniques, either at the conception stage as well as for performance improvements of existing units is emphasized.

Keywords Simulated moving bed · True moving bed · Chromatographic separations · *p*-xylene · Chiral · Modelling · Simulation and optimization

1 Introduction

The study of large scale adsorptive/chromatographic separation processes is usually divided into two major classes: the cyclic batch operations, where the adsorbent bed is alternately saturated and regenerated; and the continuous systems, often performed by the continuous counter current contact between the fluid phase and the adsorbent solid phase, as zeolites (Sherman, 1984).

The use of continuous chromatographic counter current operation modes maximizes the mass transfer driving force, providing a better utilization of the adsorbent than in the traditional batch mode. Nevertheless, in this counter current operation (so-called TMB—True Moving Bed), it is necessary to circulate not only the fluid phase but also the solid. The solid motion has some disadvantages (attrition, lack of efficiency, fluid velocity limited by fluidization phenomena, etc.) and from a technical point of view, is not easy to implement.

The solution to this major problem was first proposed through an inventive way by Broughton and

P. Sá Gomes · M. Minceva · A. E. Rodrigues (✉)
Laboratory of Separation and Reaction Engineering (LSRE), Department of Chemical Engineering—Faculty of Engineering, University of Porto, Rua Dr. Roberto Frias s/n, 4200-465 Porto, Portugal
e-mail: arodrig@fe.up.pt

Table 1 Comparison of "Old" and "New" SMB units

	p-xylene separation	Chiral separations
Number of columns N_c	24	6
Column length L_c (m)	1.0	0.1
Column internal diameter D_c (m)	9.5	1.0
Particle radius R_p ($\times 10^{-3}$ m)	0.60	0.02
Aspect ratio D_c/L_c	$\approx$10	$\approx$10
Productivity $\left(\frac{kg}{m^3_{\text{adsorbent}} \cdot h}\right)$	120	1–10
Adsorbent capacity $\left(\frac{kg}{m^3_{\text{adsorbent}}}\right)$	200	10

Gerhold (1961); using simple fixed bed columns the solid movement is simulated by a synchronous shift of all inlet and outlet ports in the direction of the fluid flow. This simulated solid motion lead to the Simulated Moving Bed (SMB) concept firstly implemented by the UOP Inc. in the "Sorbex®" processes, the very first successful commercial large-scale SMB units. Examples from the petrochemical industries are the "Parex®" units for the separation of p-xylene from its isomers on zeolites, the "Molex®" for the separation of n-paraffins from branched and cyclic hydrocarbons, the "Olex®" process to separate olefins from parafins. Examples from sugar industries include the "Sarex®" for the separation of fructose from the corn syrup with dextrose and polysaccharides on polystyrene-divinylbenzene resins in calcium form. Until the 90 s the major implementation of the SMB technology continued to be in the petrochemical separation field with more than 100 industrial plants. The biggest SMB plant in the world (South Korea) is based on the "Eluxyl®" process (Pavone and Hotier, 2000), designed by Axens/IFP (Institut Français du Pétrole), for the separation of *p*-xylene; it has 24 columns with more than 9.0 m of i.d. and higher than 1 m.

With the development of HPLC for the preparative separation of fine chemicals in the earlier 70 s, smaller stationary phase particles (10 to 40 μm) and consequently the use of shorter columns operating at higher pressure were used. Chromatographic processes became more interesting for the pharmaceutical industry, to meet product purities constraints imposed by the pharmaceutical and food regulatory organizations Examples are the separation of enantiomers and active compounds (enzymes, peptides, antibiotics, etc...). in the biotechnological industry. However, preparative chromatography has some limitations of dilution and consequently low productivity values.

The application of the SMB concept to HPLC chromatographic separations in the earlier 90 s, led to the second "boom" on the SMB technology applied now to the fine chemistry separations (Nicoud, 1999a,b; Rodrigues and Pais, 2004). The scale is much smaller than that used in the petrochemical field. Some of the design as performance parameters are presented in Table 1, where it is interesting to note that some design parameters relations are the same in the "old" and "new" SMB applications; for example the aspect ratio between column diameter and column high is roughly 10.

During these last 10 years, the application of SMB technology to the fine chemistry area, resulted in a considerable amount of technological and scientific advances, and is now an important research topic of some academic/industrial groups around the globe.

All this interest on the SMB technology led to the formulation of theories, methodologies and new concepts as well as the design of non conventional SMB operation modes, as the introduction of the asynchronous inlet/outlet ports shift as proposed by Adam et al. (2000) and Ludemman-Hombouger et al. (2000) on the Varicol® technique. Other new ideas are presented in a latter section (Non-Conventional SMB operating modes).

The optimization and design of SMB units has also been addressed in some important publications to the SMB field. The application of the Equilibrium Theory (DeVault, 1943; Klein et al., 1967; Tondeur and Klein, 1967; Helfferich, 1967; Helfferich and Klein, 1970; Rhee et al., 1970) by Storti et al. (1989, 1993), Mazzotti et al. (1997), Chiang (1998) and Migliorini et al. (2000) led to the formulation of the "Triangle Theory." This is an important methodology in the SMB design field; it allows one to find a feasible zone where separation is obtained for both linear or non-linear isotherms. However, since it is based on the Equilibrium Theory, all mass transfer effects are ignored. Another methodology is the "Separation Volume", introduced by Azevedo and Rodrigues (1999), Minceva and Rodrigues (2002) and Rodrigues and Pais (2004). It is based in a model, including mass transfer resistances as well as the influence of the regeneration zones operating parameters onto the separation performance. Another well known design methodology is the one introduced by Ma and Wang (1997), the concept of standing waves, i.e., the flow rate in each zone can be chosen so that the key concentration wave (boundary of a solute band) in each zone migrates at the same speed as the ports. As a result, all band boundaries, or waves, remain standing with respect to the ports. These theories can be useful for *a priori* selection of the operating conditions to achieve the required separation as well as good starting points as region constraints to more extensive optimization procedures. The use of powerful optimization routines as the commercial package gOPT in gPROMS from Process system enterprise working with the CVP_SS solver (Control Vector Parameterisation_Single Shooting) used in the two level optimization of a existing Parex®unit in Minceva and Rodrigues (2005) or Jumping Gene based algorithms genetic algorithms by Nasat and Gupta (2003) in the NSGA-II-JG used by Kurup et al. (2006) and Kim et al. (2003), in the design and optimization of multicomponent SMB units, allows the identification of new SMB configurations.

The application of SMB technology to multicomponent separations has also been an important research topic in the last years. The common wisdom is the simple application of SMB cascades (Wankat, 2001; Kim et al., 2003; Kim and Wankat, 2004), Nicolaos et al., 2001a, b; nevertheless, there are some non-conventional operation modes that proved to have interesting performance, as the pseudo-SMB in Mata and Rodrigues (2001) and Borges da Silva and Rodrigues (2006) presented first by Japan Organo Co. (www.organo.co.jp). The use of 5 zones SMBs (Kim et al., 2003; Kurup et al., 2006), two different adsorbents as in Hashimoto et al. (1993), two different solvents in Balannec and Hotier (1993), or a variation of the working flow rates during the switching period (Kearney and Hieb, 1992) were also proposed.

In recent years the control of SMB units has been investigated (Erdem et al., 2004a). Several reports on dynamic control strategies include nonlinear control strategies such as: (a) the input-output linearizing control, where the controller action is based on a nonlinear state estimator using the TMB model (Kloppenburg and Gilles, 1999); (b) repetitive model predictive control (RMPC) (Natajan and Lee, 2000; Abel et al., 2004; Erdem et al., 2004b). Also a model based SMB control where an optimal trajectory calculated off-line should be followed was proposed by Klatt et al., 2000. A more recent strategy based on the nonlinear wave propagation phenomena aims to control the central sections of the SMB unit by controlling the position of the concentration fronts (Schramm et al., 2001). Model predictive control (MPC) of SMB units (Morari and Lee, 1999) and design on the basis of neural networks (Wang et al., 2003) should be mentioned.

The combination of a chemical reaction and a separation process in the same unit leads, in several cases, to the improvement of reaction efficiency (Silva and Rodrigues, 2004, 2005; Lode et al., 2001; Kurup et al., 2005). The Simulated Moving Bed Adsorptive Reactor (SMBAR), is a continuous reaction/separation chromatographic process reported in literature. The esterification from acetic acid and β-phenethyl alcohol and subsequent separation of the product β-phenetyl acetate (Kawase et al., 1996), the synthesis and separation of the methanol from syngas (Kruglov et al., 1994)), or the diethylacetal synthesis (Silva and Rodrigues, 2004, 2005) are examples that show the potential of this technique.

The combination of SMB with other separation techniques, sometimes called as *hybrid-SMB* is also matter of interest. The coupling of SMB chromatography and crystallization, especially for the separation of enantiomers has been proposed and discussed in the literature (Lim et al., 1995; Blehaut and Nicoud, 1998; Lorenz et al., 2001; Strohlein et al., 2003; Amanullah et al., 2004; Strobe et al., 2004; Kaspereit et al., 2005; Amanullah and Mazzotti, 2006) among others).

After more than 40 years of developments and a new age in the last decade, the SMB appears as a key technology for chromatographic separations, applied in different fields as bioseparations (separation of sugars, desalting and proteins purification), organic molecules where many separations have been performed but only a few published and in the pharmaceutical field for the separation of enantiomers. A search in www.google.com for "Simulated Moving Bed" shows 53,700 occurrences compared with 235,000 for "Distillation Column", which indicates the relative importance of the subject. Additionally it is now possible to find SMB units from several companies with plants from the laboratory to the industrial scale. For p-xylene separation examples are UOP (Des Plaines, IL, USA)

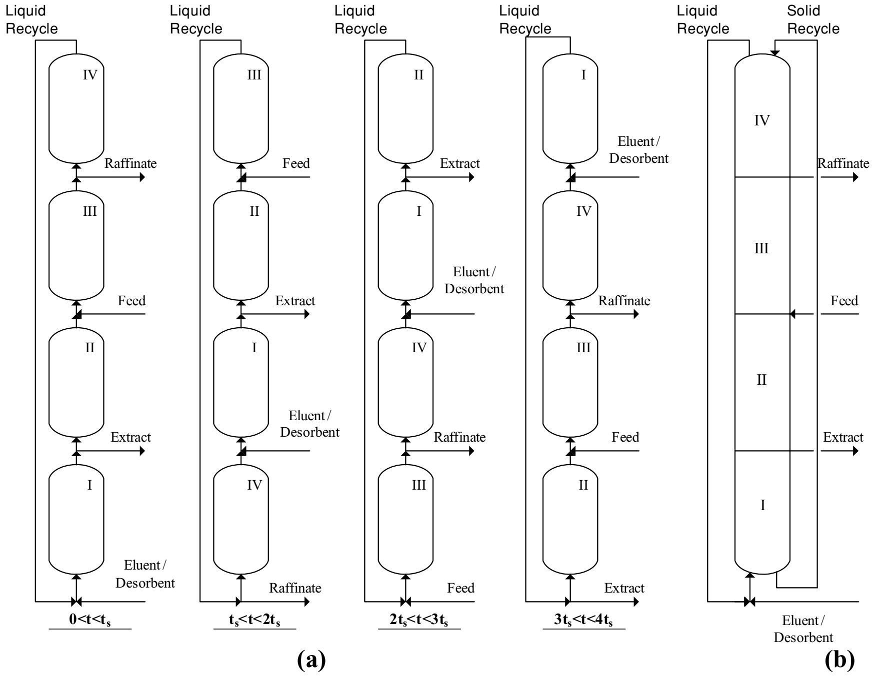

Fig. 1 (a) Schematic representation of a 4 columns SMB unit operating over a complete cycle, from 0 to $4t_s$ (with t_s representing the ports switch time) and (b) "4 columns length" TMB unit

Parex®, IFP-Axens's Eluxyl® and Toray's Amorax; for industrial chiral separations units are mainly from NOVASEP, (Pompey, France).

2 Modelling methodologies and operation principles

2.1 Operating procedure

As already mentioned the SMB *modus operandi* (Fig. 1(a)) was inspired in the continuous counter current TMB process (Fig. 1(b)), and the equivalence between the practical and ideal concepts respectively can be and is indeed usually explored in the modelling field.

From both Fig. 1(a) and (b) it is possible to note 4 different zones, between the inlet and outlet ports. The zone 1, limited by the desorbent and the extract ports, is the solid regeneration zone. The separation zones 2 and 3 are limited by the extract and feed ports, and feed and raffinate ports, respectively. The more retained species is directed for the extract collection point while the less retained species is directed to the raffinate collection point. The zone 4 is the desorbent regeneration zone, located between the raffinate and desorbent ports.

2.2 Design methodology

It is possible to simulate both the SMB as the TMB using a more complete model, detailing the particle diffusion and/or film mass transfer (the detailed particle model) as stated for reactive systems in Sá Gomes et al. (2006), or by approximation of the intraparticle mass transfer rate with the Linear Driving Force (LDF) model of Glueckauf (1965). This second methodology proved to be adequate to describe experimental results and is used by the majority of researchers in the field.

To achieve separation between the two species it is necessary to define appropriated operating conditions, i.e. the internal flow rates for the fluid phase and the SMB switch time (representing the equivalent solid velocity in the TMB model). Usually one operating parameter combines fluid and solid velocities in each zone. Examples of similar operating parameters are the Hashimoto's β_j (Hashimoto et al., 1993), the γ_j established by Ruthven group (Ruthven and Ching, 1989), or the m_j from Morbidelli and his co-workers (Migliorini et al., 2000; Morbidelli and Mazzotti, 2002); in this work γ_j, the fluid and solid interstitial velocities ratio in zone j will be used.

With the TMB model it is possible to solve the steady state case where model equations are reduced to a simple ODE system, presenting in fact a reasonable

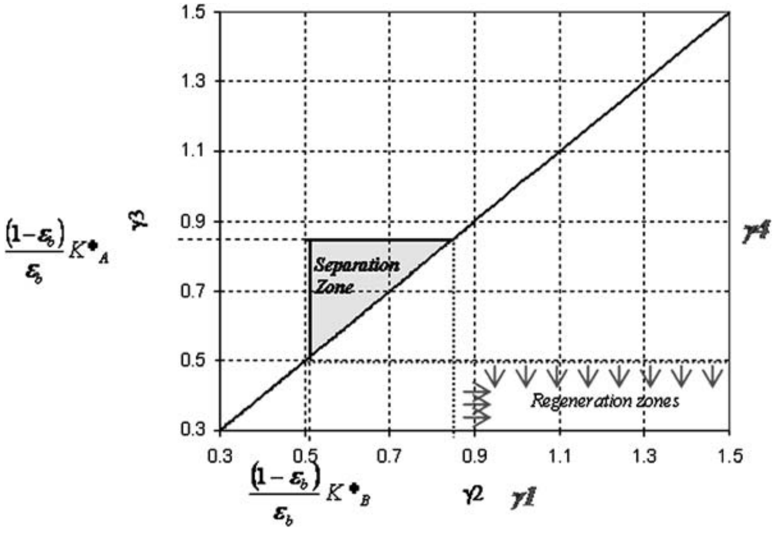

Fig. 2 Equilibrium theory separation and regeneration for linear isotherms as in Leão and Rodrigues (2004), where K_i^* represents the Henry constant for linear adsorptions isotherms

agreement with the real SMB unit when a large number of columns is considered. Nevertheless, the two modelling strategies are here used: one represents a true counter-current system (TMB) and is applied in the simulation of a Parex® unit of 24 columns and the other simulates the real SMB system directly in the case of a chiral separation with 8 columns, and a 5 columns Varicol® example. It is also worth noting that the time-dependence of the boundary conditions in the SMB model leads to a cyclic steady-state (CSS), instead of a steady-state achieved for the TMB model.

To recover a more retained species (A) in the extract stream and a less retained one (B) in the raffinate port, the operating parameters are set in a way that in the zone 1 the more retained species is directed upwards, providing the solid regeneration, in zones 2 and 3 the species movement is downwards for the more retained and upwards for the less retained, and for zone 4 the species movement is with the solid, i.e., downwards for the less retained species, cleaning the eluent to be recycled. These specifications on the operating parameters lead to the general constraints:

$$\begin{aligned}
&\gamma_1 > \frac{1-\varepsilon_b}{\varepsilon_b}\frac{\langle q_{A1}\rangle}{C_{bA1}}\\
&\frac{1-\varepsilon_b}{\varepsilon_b}\frac{\langle q_{B2}\rangle}{C_{bB2}} < \gamma_2 < \frac{1-\varepsilon_b}{\varepsilon_b}\frac{\langle q_{A2}\rangle}{C_{bA2}}\\
&\frac{1-\varepsilon_b}{\varepsilon_b}\frac{\langle q_{B3}\rangle}{C_{bB3}} < \gamma_3 < \frac{1-\varepsilon_b}{\varepsilon_b}\frac{\langle q_{A3}\rangle}{C_{bA3}}\\
&\gamma_4 < \frac{1-\varepsilon_b}{\varepsilon_b}\frac{\langle q_{B4}\rangle}{C_{bB4}}
\end{aligned} \qquad \text{(1a–d)}$$

where C_{bij} is the bulk fluid phase concentration of species i in zone j, $\langle q_{ij}\rangle$ is the average solid concentration of species i in zone j and ε_b the bed porosity. The relation $\frac{\langle q_{ij}\rangle}{C_{bij}}$ can now be treated by one of the two more common strategies: (a) assuming equilibrium theory where the adsorption equilibrium is established everywhere at every time resulting in a feasible separation region formed by the above constraints (1b) and (1c), which in the case of linear isotherms takes the shape of a rectangular triangle in the ($\gamma_2 \times \gamma_3$) plane as in Fig. 2, or a triangle shaped form with rounded lines in non linear isotherms case; and (b) using the “Separation Volume” methodology, where all mass transfer resistances are taken into account (see Fig. 3 for the separation region), plus the separation/regeneration study is carried for three different zones (2, 3 and 1) or (2, 3 and 4) allowing the analysis of solvent consumption or solid recycling.

2.3 Numerical solution

The numerical solutions for the different model equations were obtained using the gPROMS v3.0.0 a commercial package from Process Systems Enterprise. The mathematical models are constituted by systems of PDE (Partial Differential Equations), ODE (Ordinary Differential Equations) and AE (Algebraic Equations), that were solved by applying one of the discretization methods available in gPROMS, namely OCFEM (Orthogonal Collocation on Finite Elements) with 2 collocation points per element, 50 elements in each column for the axial coordinate. After the

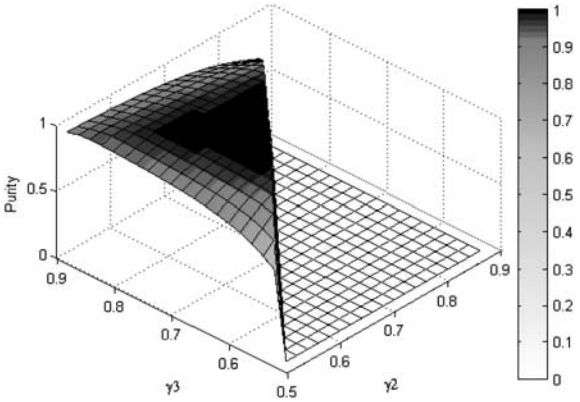

Fig. 3 Separation region for linear isotherms in presence of mass transfer resistances

axial discretization step, the time integration is performed by the ordinary differential equation solver SRADAU a fully-implicit Runge-Kutta method that implements a variable time step, the resulting system is then solved by the gPROMS BDNSOL (Block decomposition NonLinear SOLver) www.psenterprise.com.

2.4 Performance parameters

The performance parameters are: purity, recovery, desorbent consumption and productivity. The SMB outlet streams must satisfy purity and recovery specifications. The definitions of extract purity (*PUX*, %), raffinate purity (*PUR*, %), recovery of species A in the extract (REX^A, %), recovery of species B in the raffinate (RER^B, %), and the unit productivity in terms of A in the extract (PR_X^A) or species B in raffinate (PR_R^B), that characterize each SMB unit performance are:

$$PUX^A(\%) = \frac{C_{b_A}^X}{\sum_{k=1}^{NC} C_{b_k}^X} \times 100 \tag{2}$$

$$REX^A(\%) = \frac{Q_X C_{b_A}^X}{Q_F C_A^F} \times 100 \tag{3}$$

$$PR_X^A = \frac{Q_X C_{b_A}^X}{V_{\text{ads}}} = \frac{REX^A \cdot Q_F C_A^F}{V_{\text{ads}}} \tag{4}$$

where Q_X and Q_F are the extract and feed flow rates, respectively and V_{ads} the adsorbent volume. Similar definitions hold for the raffinate.

3 The "Old" applications to the SMB concept

The SMB technology first appeared in the petrochemical industry and in the sugar industries as the solution to the so-called difficult separations. An example is the Parex® process from UOP, one of the Sorbex® processes, for the separation of *p*-xylene (A) from its C_8 aromatic isomers *m*-xylene (B), *o*-xylene (C) and Ethylbenzene (D) using *p*-Diethylbenzene as desorbent (E). Until the introduction of the Parex® process, *p*-xylene was produced by crystallization; the eutectic composition and slurry solids limitation from crystallization process allowed recoveries of 60–65%. The mother liquor, with the unrecovered *p*-xylene and the other isomers was sent to an isomerisation unit where the isomers were re-equilibrated. The isomerate was then combined with a fresh feed source and recycled to the crystallizer. The Parex® process with *p*-xylene recoveries of 90–95% providing significant economic benefits. Over the years several improvements on the initial Parex®process were noted and other processes like Eluxyl® from Axens/IFP and Toray's Aromax appeared being now possible the recovery of *p*-xylene at high purity of 99.5% to 99.9%.

3.1 Simulation of a simplified Parex® unit

The Parex® unit studied by Minceva and Rodrigues in several published works (Minceva and Rodrigues, 2002, 2003, 2004b) is here used as case study for an "old" SMB application. The system according to the Minceva (2004a) can be well represented by the Langmuir Competitive isotherm model as in Eq. (5),

$$q_{ij}^* = \frac{q_{mi} K_i \langle C_{pij} \rangle}{1 + \sum_{i=1}^{Nc} K_i \langle C_{pij} \rangle} \tag{5}$$

where q_{mi} is the adsorbed phase saturation concentration of component i and K_i the Langmuir adsorption constant for species i and q_{ij}^* is the adsorbed phase concentration of component i in zone j in equilibrium with the average pore concentration $\langle C_{pij} \rangle$. The adsorption equilibrium data of the single *p*-xylene, *o*-xylene and ethylbenzene on Ba exchanged faujasite zeolite in liquid phase at 180°C and 9 bar was determined experimentally in a batch mode as in Minceva and Rodrigues (2004b). The adsorption parameters for m-xylene are similar to those for *o*-xylene in this type of zeolites

Table 2 Parameters of Langmuir adsorption equilibrium isotherms

Component	K_i ($\mathrm{m}^3 \cdot \mathrm{kg}^{-1}$)	q_{mi} ($\mathrm{kg} \cdot \mathrm{kg}^{-1}{}_{\mathrm{adsorbent}}$)
(A) *p*-xylene	1.9409	0.1024
(B) *m*-xylene	0.8884	0.0917
(C) *o*-xylene	0.8884	0.0917
(D) ethylbenzene	1.0263	0.0966
(E) *p*-diethylbenzene	1.2000	0.1010

Table 3 Parex® unit characteristics and model parameters

Model parameters	SMB columns
$Pe_j = 1000$	$N_c = 24 \quad n_j = [6 \;\; 9 \;\; 6 \;\; 3]$
$\varepsilon_b = 0.387$; $\varepsilon_p = 0.37$	$L_c = 1.135\,\mathrm{m}$
$R_p = 0.031\,\mathrm{cm}$	$D_c = 4.117\,\mathrm{m}$
	SMB operating conditions
$\rho_p = 1.480\,\mathrm{g{\cdot}cm^{-3}}$	
$\rho_{f(A,B,C,D,E)} = 0.724\ \mathrm{g{\cdot}cm^{-3}}$	$C_A^F = 23.6\,\mathrm{wt\%}$; $C_B^F = 49.7\,\mathrm{wt\%}$
	$C_C^F = 12.7\,\mathrm{wt\%}$; $C_D^F = 14.0\,\mathrm{wt\%}$
	$C_E^{\mathrm{Desorbent}} = 100.0\ \mathrm{wt\%}$
$k_{\mathrm{LDF}_{(A,B,C,D)}} = 8.1\,\mathrm{min}^{-1}$; $k_{\mathrm{LDF}_{(E)}} = 6.8\,\mathrm{min}^{-1}$	$t_s = 1.15\,\mathrm{min}$;
	$Q_{\mathrm{Desorbent}} = 133.657\ \mathrm{m^3{\cdot}h^{-1}}$; $Q_{\mathrm{Extract}} = 95.250\ \mathrm{m^3{\cdot}h^{-1}}$;
	$Q_{\mathrm{Feed}} = 90.000\ \mathrm{m^3{\cdot}h^{-1}}$; $Q_{\mathrm{Raffinate}} = 128.407\ \mathrm{m^3{\cdot}h^{-1}}$;
	$Q_1{}^{*} = 658.486\ \mathrm{m^3{\cdot}h^{-1}}$

Table 4 Parex® SMB and equivalent TMB zone operating conditions

Real SMB	Equivalent TMB
$\gamma_j^* = [2.158 \quad 1.846 \quad 2.141 \quad 1.720]$	$\gamma_j = [1.158 \quad 0.846 \quad 1.141 \quad 0.720]$
$Q_j^* = [658.486 \quad 563.236 \quad 653.236 \quad 524.829]\ \mathrm{m^3{\cdot}\,h^{-1}}$	$Q_j = [353.412 \quad 258.162 \quad 348.162 \quad 219.756]\ \mathrm{m^3{\cdot}h^{-1}}$
	$Q_s = 483.238\ \mathrm{m^3{\cdot}h^{-1}}$

according to Santacesaria et al. (1982). The *p*-DEB isotherm was taken from Minceva (2004a); all adsorption equilibrium parameters are presented in Table 2.

The SMB unit operating conditions and model parameters are presented in Tables 3 and 4, where the density of the liquid (fluid phase), ρ_f, is considered to be constant and similar to the density value for the p-diethylbenzene (724 $\mathrm{kg{\cdot}m^{-3}}$) at 180 °C and 9 bar as well as constant apparent solid density ρ_p.

When a large number of columns is present it is wise to use the equivalent TMB model as an approximation to the SMB unit; therefore, this approach will be used with a LDF approximation for the intraparticle mass transfer rate.

The analogy between SMB and the TMB is possible by the introduction of the relative velocity concept $u_j^* = u_j + u_s$, where u_j is the fluid interstitial velocity in the TMB model and u_j^* the interstitial velocity in the SMB unit and u_s, the solid velocity in the TMB. The solid velocity is evaluated from the switch time interval value t_s in the SMB as $u_s = \frac{L_c}{t_s}$. The internal flow-rates in both models are not the same, but related by $Q_j^* = Q_j + \frac{\varepsilon_b V_c}{t_s}$, where Q_j^* and Q_j represent the internal liquid flow-rates in the SMB and TMB, respectively and V_c the column volume. For the TMB model the nodes balances are in Table 5, with C_i^F the species i feed inlet concentration, and $C_i^{\mathrm{Desorbent}}$ the species i desorbent concentration inlet. The model is formulated considering a convective fluid movement with axial dispersion, with counter current solid plug flow, negligible thermal effects, constant values for the bed void fraction ε_b and particle porosity ε_p, axial dispersion coefficient D_{bj}, particle radius R_p, constant values for the flow rates/interstitial velocities in each zone, and

Table 5 TMB nodes balances

$j = 1\text{: } C_{bi(4,x=1)} = \frac{u_1}{u_4} C_{bi(1,x=0)} - \frac{u_{\text{Desorbent}}}{u_4} C_i^{\text{Desorbent}}$	(6a)	$u_1 = u_4 + u_{\text{Desorbent}}$	(7a)
$j = 2{,}4\text{: } C_{bi(j-1,x=1)} = C_{bi(j,x=0)}$	(6b)	$u_2 = u_1 - u_{\text{Extract}}$	(7b)
$j = 3\text{: } C_{bi(2,x=1)} = \frac{u_3}{u_2} C_{bi(3,x=0)} - \frac{u_{\text{Feed}}}{u_2} C_i^F$	(6c)	$u_3 = u_2 + u_{\text{Feed}}$	(7c)
		$u_4 = u_3 - u_{\text{Raffinate}}$	(7d)

Table 6 TMB model equations with LDF approach

i. In a volume element of the bulk fluid phase,

$$\frac{\partial C_{bij}}{\partial \theta} = \frac{\gamma_j}{n_j} \left\{ \frac{1}{Pe_j} \frac{\partial^2 C_{bij}}{\partial x^2} - \frac{\partial C_{bij}}{\partial x} - \frac{(1-\varepsilon_b)}{\varepsilon_b} k_{p_{ij}} \left(C_{bij} - \left\langle C_{pij} \right\rangle \right) \right\} \tag{8}$$

ii. and for the adsorbent phase,

$$\rho_p \frac{\partial q_{ij}}{\partial \theta} + \varepsilon_p \frac{\partial \left\langle C_{pij} \right\rangle}{\partial \theta} = \frac{1}{n_j} \left[\rho_p \frac{\partial q_{ij}}{\partial x} + \varepsilon_p \frac{\partial \left\langle C_{pij} \right\rangle}{\partial x} \right] + \frac{\gamma_j}{n_j} k_{p_{ij}} \left(C_{bij} - \left\langle C_{pij} \right\rangle \right) \tag{9}$$

with the initial conditions and the Danckwerts (1953) boundary conditions, previously mentioned in Langmuir's work (1908),

- $$\begin{cases} C_{bij}(x, 0) = 0; \\ \left\langle C_{pij}(x, 0) \right\rangle = 0; \\ q_{ij}(x, 0) = 0; \end{cases} \tag{10}$$
- $$x = 0\text{: } C_{bi(j,x=0)} = C_{bij}(0, \theta) - \frac{1}{Pe_j} \left. \frac{\partial C_{bij}}{\partial x} \right|_{x=0} \tag{11a}$$
- $$x = 1\text{: } \left. \frac{\partial C_{bij}}{\partial x} \right|_{x=1} = 0 \tag{11b}$$
- $$x = 1 \begin{cases} \left\langle C_{p_{i(j,x=1)}} \right\rangle = \left\langle C_{p_{i(j+1,x=0)}} \right\rangle \\ \left\langle C_{p_{i(4,x=1)}} \right\rangle = \left\langle C_{p_{i(1,x=0)}} \right\rangle \end{cases}, \quad \text{for } j = 1{,}2{,}3; \tag{12a}$$
- $$x = 1 \begin{cases} q_{i(j,x=1)} = q_{i(j+1,x=0)} \\ q_{i(4,x=1)} = q_{i(1,x=0)} \end{cases}, \quad \text{for } j = 1{,}2{,}3; \tag{12b}$$

plus the multicomponent adsorption isotherms

$$q_{ij} = f_i \left(\left\langle C_{pij} \right\rangle, \left\langle C_{pkj} \right\rangle \right) \text{ with } k \neq i \text{ and for all species } i \text{ and in zone } j \tag{13}$$

in this case as Eq. (5).

also negligible pressure drop, leading to the model as in Table 6.

In the model equations $\langle C_{pij} \rangle$ and q_{ij} are the average concentration of species *i* in the pores and the adsorbent phase concentration, respectively; $\theta = \frac{t}{t_s}$ is the dimensionless time normalised by the SMB ports switch time t_s, $x = \frac{z}{L_j}$ the dimensionless column axial coordinate with respect to the length of zone j, $L_j = L_c n_j$; $\gamma_j = \frac{u_j}{u_s}$ the ratio between fluid and solid interstitial velocities, $Pe_j = \frac{u_j L_j}{D_{bj}}$ the Peclet number, with $t_j = \frac{L_j}{u_j}$ the fluid phase space time; and $k_{p_{ij}} = k_{\text{LDF}} \cdot t_j$ the number of intraparticle mass transfer units, based on the LDF mass transfer coefficient k_{LDF}.

The steady state solution, in terms of liquid phase bulk concentration profiles, is presented in Fig. 4, with *p*-xylene purity in the extract of 99.84%, recovery 99.26% and productivity of 68.7 $\frac{kg_{p\text{-xylene}}}{h \cdot m^3_{\text{adsorbent}}}$. These values were obtained for a simplified Parex® unit; a real UOP Parex® unit includes flushing in and flushing out lines, and therefore the performance parameters are different from those simulated here, Minceva and Rodrigues (2003).

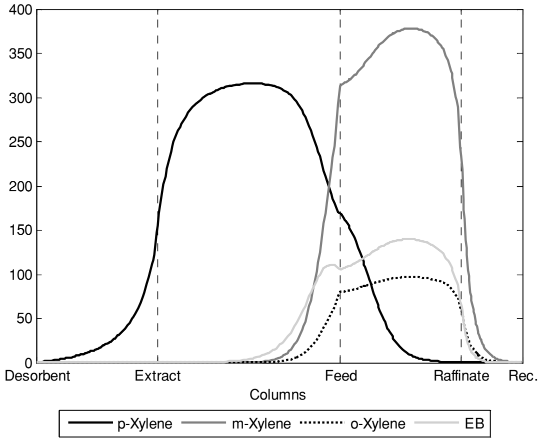

Fig. 4 Steady-state liquid phase Parex® concentration profiles

3.2 Methodology for a two level optimization of a Parex® unit

The SMB optimization field can be classified with relation to 3 categories: (i) the number of objective functions; (ii) the type of the objective functions;

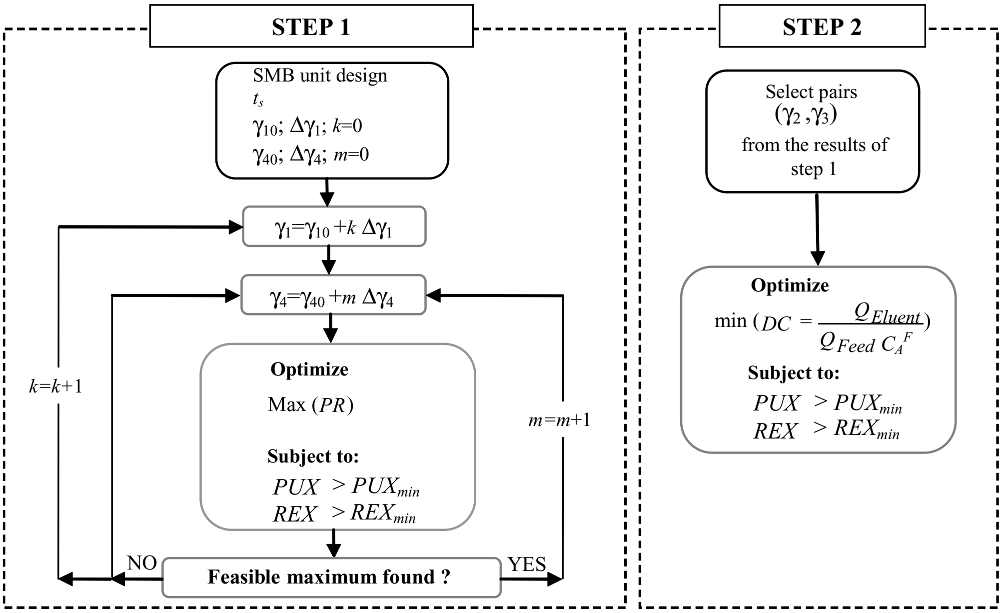

Fig. 5 Two-Level optimization of a Parex® unit, adapted from Minceva and Rodrigues (2005)

(iii) optimization of a new or an already existing SMB unit (only optimization of the operating parameters). Taking into account the number of objective functions, problems can be considered as single-objective or multiple-objective optimization. In the case of multiple-objective optimization a global optimum may not exist; there is a possibility of an entire set of optimal solutions that are equally good, the so-called Pareto Optimal Solutions.

As for the objective functions two main cases can be considered: (i) performance parameters (productivity, adsorbent requirements or desorbent/eluent consumption); (ii) separation cost. In the case (i) with optimization each objective function can lead to a different optimum solution; therefore a multi-objective functions procedure should be considered, as for case (ii) all those different performance parameters could be homogenized/normalized by the separation cost, where separation problem independent costs (wages, labour, maintenance, etc.) and the separation cost dependent costs (adsorbent, plant, desorbent/eluent consumption, desorbent/eluent recycling, feed losses, etc.) are taken into account, and the weight given to each factor is of importance and some times difficult to characterize.

In this work the example of a two-level optimization procedure to an already existing Parex® unit is presented (Minceva and Rodrigues, 2005); a detailed state of the art of SMB optimization can be found in that reference.

The base algorithm can be described as in Fig. 5, where it is shown that for a first set of γ_1 and γ_4 parameters the gPROMS gOPT is used to find the best productivity solutions by changing the separation zone operating parameters, γ_2 and γ_3, that meet *PUX* and *REX* constraints. The second step is the minimization of desorbent consumption working now with the zone 1 and 4 operating parameters, γ_1 and γ_4; for each selected pairs of γ_2 and γ_3 obtained from the first step the optimum values of γ_1 and γ_4 are found.

4 The "New" applications to the SMB concept

A well known example for a "new" SMB application is the separation of racemic mixtures of chiral drugs in the pharmaceutical industry. Many chiral drugs are produced as a 50–50% mixture of the two enantiomers, the racemate. The problem is that those two enantiomers can often have different biological activity. Therefore, it becomes important the separation of the target isomer from the other that can be inactive or have an adverse effect. There are two different approaches to obtain pure enantiomers compounds: (a) preparing the racemic material and then the separation

Table 7 SMB unit characteristics and model parameters

Model Parameters	SMB Columns
$Pe_c = 1000$	$N_c = 8 \quad n_j = [2\ \ 2\ \ 2\ \ 2]$
ε_b=0.4;	$L_c = 9.9\times10^{-2}$ m
$R_p = 2.25 \times 10^{-5}$ m	$D_c = 2.6\times10^{-2}$ m
	Classic SMB Operating Conditions
$k_{\mathrm{LDF}} = 0.33\ \mathrm{s}^{-1}$	${C_A}^F = 5$ g·l^{-1}; ${C_B}^F = 5$ g·l^{-1} $t_s = 198$ s; $Q_{\mathrm{Eluent}} = 12.038$ ml·min^{-1}; $Q_{\mathrm{Extract}} = 8.990$ ml·min^{-1}; $Q_{\mathrm{Feed}} = 0.956$ ml·min^{-1}; $Q_{\mathrm{Raffinate}} = 4.004$ ml·min^{-1}; $Q_4 = 21.800$ ml·min^{-1}.

Table 8 Classic SMB and equivalent TMB zone operating conditions

Real SMB	Equivalent TMB
$\gamma_j^* = [5.311\quad 3.900\quad 4.050\quad 3.422]$	$\gamma_j = [4.311\quad 2.900\quad 3.050\quad 2.422]$
$Q_j^* = [33.838\quad 24.848\quad 25.804\quad 21.800]$ ml·min^{-1}	$Q_j = [27.467\quad 18.477\quad 19.433\quad 15.429]$ ml·min^{-1}
	$Q_s = 9.557$ ml·min^{-1}

Table 9 SMB nodes balances

$j = 1$: $C_{bi(4,x=1)} = \frac{u_1^*}{u_4^*} C_{bi(1,x=0)}$	(14a)	$u_1^* = u_4^* + u_{\mathrm{Eluent}}$	(15a)
$j = 2{,}4$: $C_{bi(j-1,x=1)} = C_{bi(j,x=0)}$	(14b)	$u_2^* = u_1^* - u_{\mathrm{Extract}}$	(15b)
		$u_3^* = u_2^* + u_{\mathrm{Feed}}$	(15c)
$j = 3$: $C_{bi(2,x=1)} = \frac{u_3^*}{u_2^*} C_{bi(3,x=0)} - \frac{u_{\mathrm{Feed}}}{u_2^*} C_i^F$	(14c)	$u_4^* = u_3^* - u_{\mathrm{Raffinate}}$	(15d)

or (b) asymmetric synthesis of the target enantiomer. The second approach has been widely used; nevertheless, the number of stages and the cost of all enantiomeric reagents needed would decrease the economical benefits and therefore the separation of racemate performed by SMB technology is attractive.

The case study here presented is the same as in Rodrigues and Pais (2004), considering the chromatographic resolution of a racemic mixture of chiral epoxide enantiomers (Sandoz Pharma, Basel, Switzerland), with microcrystalline cellulose triacetate particles (Merck, Darmstadt, Germany) with 45 μm diameter as chiral stationary phase, and pure methanol as eluent. The adsorption equilibrium isotherms measured at 25°C and represented by the linear plus Langmuir competitive model in terms of retained concentration in the particles are:

$$q_{Aj}^* = 1.35C_{bAj} + \frac{7.32 \cdot 0.163C_{bAj}}{1 + 0.163C_{bAj} + 0.087C_{bBj}}$$

$$q_{Bj}^* = 1.35C_{bBj} + \frac{7.32 \cdot 0.087C_{bBj}}{1 + 0.163C_{bAj} + 0.087C_{bBj}}$$

with q_{ij}^* in $g \cdot l_{\mathrm{adsorbent}}^{-1}$ and C_{bij} in $g \cdot l^{-1}$.

The ratio of interstitial velocities in SMB or TMB (γ_j^* or γ_j) for zones 1 and 4 were kept constant and far from the critical values for total solid and eluent regeneration, respectively given by the equilibrium theory. For the zones 2 and 3 the interstitial velocity ratios were taken from the analysis presented by Rodrigues and Pais based on the ($\gamma_3 \times \gamma_2$) separation region for a 99.0% purity criterion with mass transfer coefficient of $k_{\mathrm{LDF}} = 0.33\ \mathrm{s}^{-1}$; a summary of operating conditions and model parameters is presented in Tables 7 and 8.

This separation is performed with a SMB unit of 8 columns and therefore for simulation purposes the SMB model will be used. In the real SMB model each column plays different functions during a whole cycle, depending on its location. After each switch time t_s the boundary conditions for each column are synchronously changed, respecting always the nodes mass balances as shown in Table 9, where u_j^* is the interstitial velocity in the zone j of the SMB. The SMB model is formulated considering a convective fluid movement with axial dispersion, negligible thermal effects, constant values for the bed void fraction ε_b, axial dispersion coefficient D_{bj}, particle radius R_p, constant values for the flow rates/interstitial velocities in each zone, and

Table 10 SMB model equations with LDF approach

i. In a volume element of the bulk fluid phase,

$$\frac{\partial C_{bic}}{\partial \theta} = \gamma_j^* \left\{ \frac{1}{Pe_c} \frac{\partial^2 C_{bic}}{\partial x^{*2}} - \frac{\partial C_{bic}}{\partial x^*} \right\} - \frac{(1-\varepsilon_b)}{\varepsilon_b} k_{p_{ic}}^* \left(q_{ic}^* - \langle q_{ic} \rangle \right) \tag{16}$$

ii. in the "adsorbent–phase",

$$\frac{\partial \langle q_{ij} \rangle}{\partial \theta} = k_{p_{ic}}^* \left(q_{ic}^* - \langle q_{ic} \rangle \right) \tag{17}$$

with the respective initial and boundary conditions,

- $$\begin{cases} C_{bic}\,(x^*, 0) = 0; \\ \langle q_{ic}\,(x^*, 0) \rangle = 0; \end{cases} \tag{18}$$
- $$x^* = 0\colon C_{bi(c,x^*=0)} = C_{bi}(0, \theta) - \frac{1}{Pe_c} \left. \frac{\partial C_{bic}}{\partial x^*} \right|_{x^*=0} \tag{19a}$$
- $$x^* = 1\colon \left. \frac{\partial C_{bic}}{\partial x^*} \right|_{x^*=1} = 0 \tag{19b}$$

and the adsorption equilibrium isotherm as defined in Eq. (13):

also negligible pressure drop. Therefore transient mass balances are performed to each species *i* in each column *c*, as in Table 10.

Now $x^* = \frac{z}{L_c}$ is the dimensionless column axial coordinate with respect to the column length L_c; $\langle q_{ic} \rangle$ the average adsorbed phase concentration of species *i*; $\gamma_j^* = \frac{u_j^*}{u_s}$ the ratio between fluid and equivalent solid interstitial velocities in SMB model, $Pe_c^* = \frac{u_j^* L_c}{D_{bj}}$ Peclet number, and $k_{p_{ic}}^* = k_{\mathrm{LDF}} \cdot t_s$ the number of intraparticle mass transfer units.

Figure 6(a) and (b) show the concentration histories for extract and raffinate respectively, until the CSS is reached. In Fig. 7(a) and (b) the detailed histories over a switch time period are shown for both species in the extract and raffinate at CSS.

The purity of species A in the extract of 99.10% and the purity of B in the raffinate is 100.00%. The recovery of A in extract is 100.00% and the recovery of B in the raffinate is 99.10%. The productivity is 0.568 $\frac{kg_A}{h \cdot m^3_{\text{adsorbent}}}$ and 0.563 $\frac{kg_B}{h \cdot m^3_{\text{adsorbent}}}$. The productivity in chiral

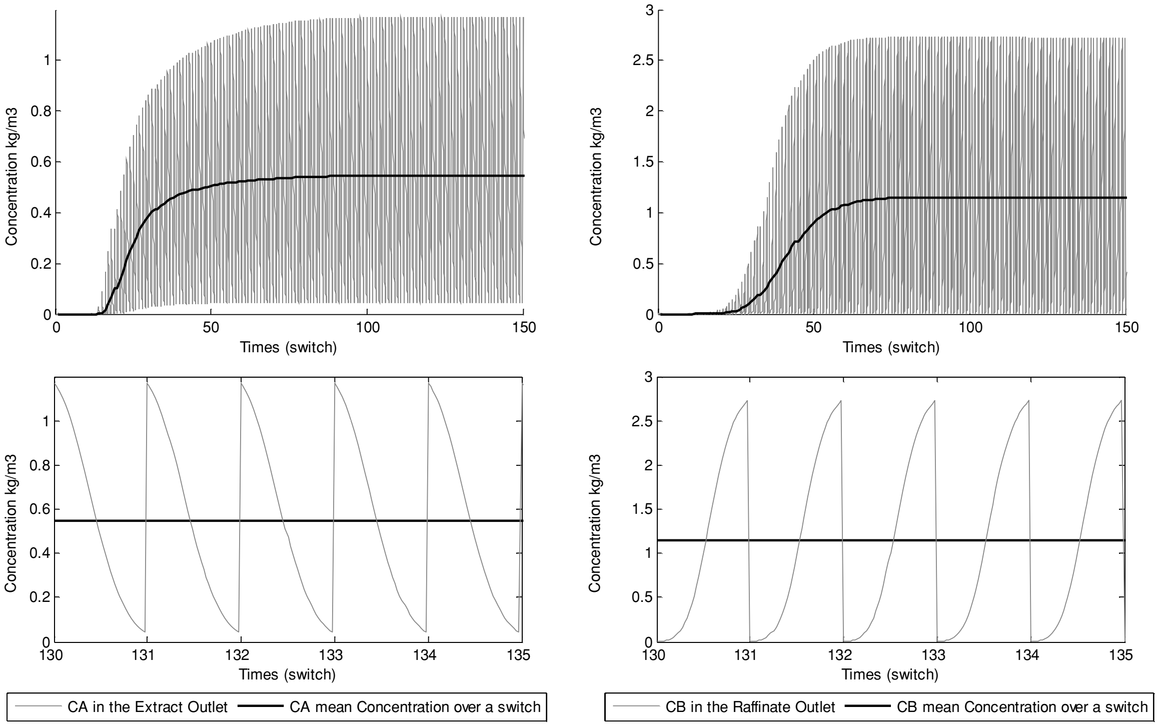

(a) (b)

Fig. 6 Concentration history C_{bA} in the extract (a) and C_{bB} in the raffinate (b)

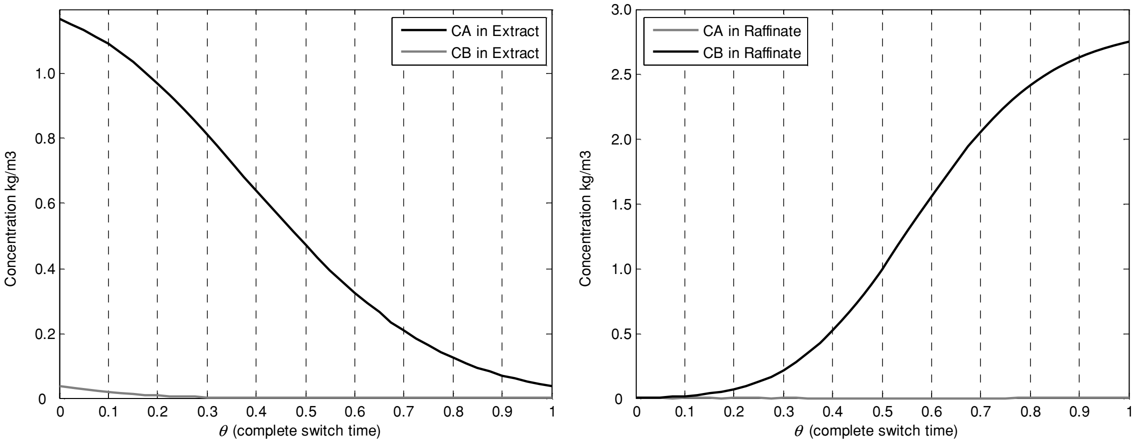

(a) (b)

Fig. 7 Concentration histories in the extract (a) and raffinate (b) during a switch time at CSS

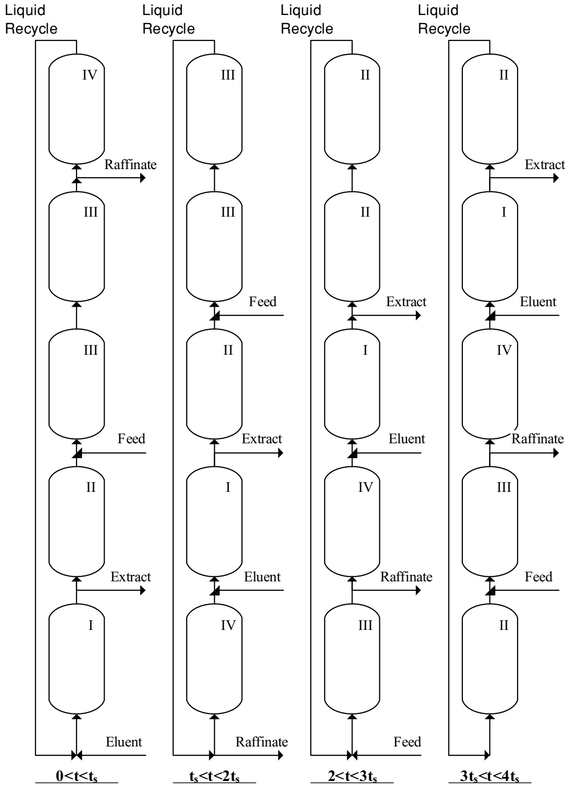

Fig. 8 Varicol® [1–1.5–1.5–1] scheme, in terms of standard SMB units [1–1–2–1] during the first half of time switch and [1–2–1–1] during the second half of time switch

separations is much lower than in the "old" Parex® application; this is mainly a result of lower adsorbent capacity of chiral packing.

5 Non conventional SMB operating modes

Until now it has only been considered the operation of the standard SMB, where each zone has a fixed number of columns, and there is no variation on the pre-established inlet/outlet flowrates and switching time. In the last years some "non-conventional" SMB operating modes were proposed providing more flexibility in the design and more efficient units.

5.1 Asynchronous SMB, the Varicol® process

The Varicol® process (Adam et al., 2000 and Ludemman-Hombouger et al., 2000), became one of the more studied and used processes of the so-called non-conventional SMB; instead of a fixed unit configuration, with constant zones length, the Varicol® operation mode provides a flexible use of columns, by the implementation of asynchronous inlet/outlet ports shift. As illustrated in Fig. 8, for the 5 columns [1 1.5 1.5 1] Varicol® (following the Ludemman-Hombouger et al. (2000) notation [N_{C1} N_{C2} N_{C3} N_{C4}] where N_{Cj} is the average number of columns contained in zone j during a switch time period), the 2nd and 3rd zones have variable length since the interior column is half of the time switch being used as a 3rd zone column and the remaining time as a 2nd zone column. The methodology can be applied to all zones, both in the separation and regeneration zones.

The Varicol® operation mode presented in this work, based in Pais and Rodrigues (2003), is designed for the

Table 11 SMB unit characteristics and parameters

Model parameters	SMB columns
$Pe_c = 1600$	$N_c = 5\ [1\ \ 1.5\ \ 1.5\ \ 1]$
$\varepsilon_b = 0.4$; $\varepsilon_p = 0.45$	$L_c = 15.84\times10^{-2}$ m
$R_p = 2.25\times10^{-5}$ m	$D_c = 2.6\times10^{-2}$ m
	SMB operating conditions
$k_{\mathrm{LDF}} = 0.4\ \mathrm{s}^{-1}$	$\mathrm{C}_A{}^F$=5 kg·m^{-3}; $\mathrm{C}_B{}^F$ = 5 kg·m^{-3} $t_s = 317$ s; $Q_s = 0.159\times10^{-6}$ m^3·s^{-1} $Q_{\mathrm{Eluent}} = 0.417\times10^{-6}$ m^3·s^{-1}; $Q_{\mathrm{Extract}} = 0.289\times10^{-6}$ m^3·s^{-1}; $Q_{\mathrm{Feed}} = 0.011\times10^{-6}$ m^3·s^{-1}; $Q_{\mathrm{Raffinate}} = 0.139\times10^{-6}$ m^3·s^{-1}; $Q_4 = 0.296\times10^{-6}$ m^3·s^{-1}.

Table 12 SMB and equivalent TMB zone operating conditions

Real SMB	Equivalent TMB
$\gamma_j^* =[6.722\ \ 4.000\ \ 4.100\ \ 2.793]$	$\gamma_j =[5.722\ \ 3.000\ \ 3.100\ \ 1.793]$
$Q_j^* =[0.713\ \ 0.424\ \ 0.435\ 0.296]\times10^{-6}$ m^3·s^{-1}	$Q_j = [0.607\ \ 0.318\ \ 0.329\ 0.190]\times10^{-6}$ m^3·s^{-1}
	$Q_s = 0.159\times10^{-6}$ m^3·s^{-1}

same chiral resolution already presented, and numerically solved using the same SMB model with LDF approach, for a small number of columns, 5. The *modus operandi* is shown in Fig. 8 and the operating parameters and unit characteristics are given in Tables 11 and 12.

Simulation results of the Varicol® unit using the SMB model with LDF approach are presented in Fig. 9(a) and (b). Purity of A in the extract is 99.62% and the purity of B in the raffinate is 99.98%.

Recoveries of A and B are 99.98% and 99.63%, respectively and productivities are 0.75 $\frac{kg_A}{h\cdot m^3_{\text{adsorbent}}}$ and 0.75 $\frac{kg_B}{h\cdot m^3_{\text{adsorbent}}}$.
As can be observed this operation mode is able to compete with standard SMB units; it shows higher productivity and the same purities and recovery performance. Pais and Rodrigues (2003) compared the [1 1.5 1.5 1] Varicol® unit here presented with various SMB configurations [1 2 1 1], [1 1 2 1] and [1 2 2 1]; the 5-column Varicol® performance was comparable with the standard 6 columns SMB and better than that of the 5 columns SMB .

5.2 Non-conventional SMB operating modes

The modulation of the feed flow rate was proposed by Morbidelli and Mazzotti (2002) and Zhang et al. (2003) in their PowerFeed technique and the variable feed concentration was suggested by Schramm et al. (2002) and (2003) in the Modicon operation mode. These operating modes provide more degrees of freedom than the classical SMB process and allow more room for optimization.

Another interesting non-conventional SMB operating modes are: the M3C process patented by Bailly et al. (2004), Abdelmoumen et al. (2006), here called as Enriched Extract operation (EE-SMB) (Paredes et al., 2006), in which a portion of the extract product is concentrated and then re-injected into the SMB at the same collection point; the semicontinous two-zone SMB/chromatography as in Hur and Wankat (2005) and (2006); and One-column Chromatograph with recycle analogous to a four-zone SMB as in Abunasser et al., (2003) or in Araújo et al., (2006).

Recently, the introduction of multi feed streams in the SMB area by analogy with distillation columns, led to the formulation of the MF (MultiFeed) operating mode presented by Kim et al. (2005) and Sá Gomes and Rodrigues (2006). This technique combined with the distillation know-how for the optimum location of multiple feeds, allows the development of new SMB processes.

Another non-conventional SMB is the Outlet Swing Stream-SMB operation mode presented by Sá Gomes and Rodrigues (2006), where the more and less retained species are collected in the extract and raffinate ports non-continuously, i.e. during a part of the time switch the more retained species is collected in the extract while the raffinate flow rate is decreased leading to the violation of the equilibrium theory constraints on zone 4; in the rest of the period the opposite procedure is

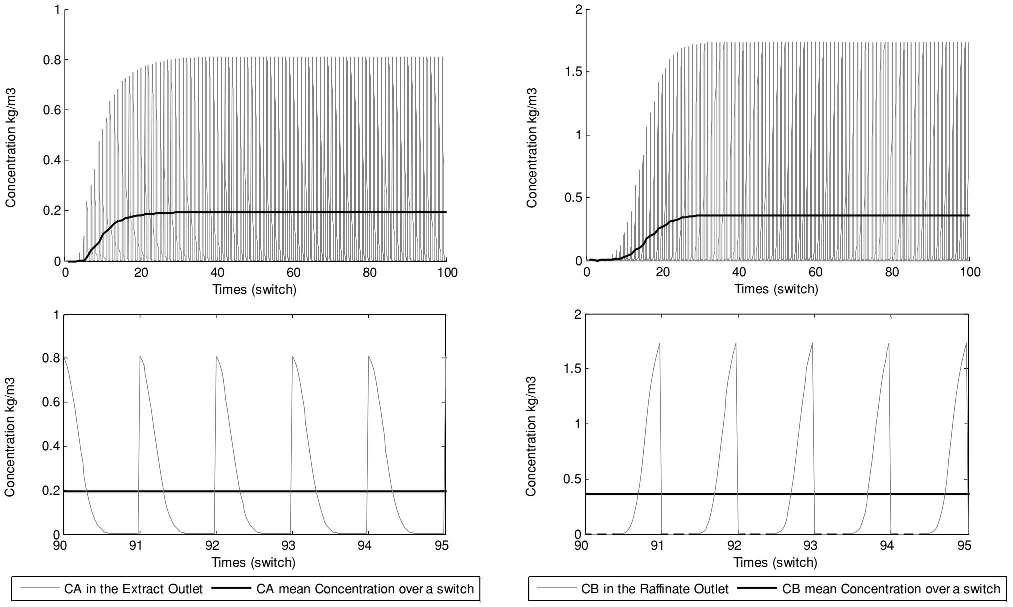

(a) (b)

Fig. 9 Varicol® concentration history C_{bA} in the extract (a) and C_{bB} in the raffinate (b)

performed. This operation mode leads to expansion and contraction of the collection and contaminating fronts increasing the distance between them.

In the multicomponent separation field it is quite interesting the operation mode introduced by the Japan Organo Co. with the JO process or Pseudo-SMB, discussed in Mata and Rodrigues (2001), Borges da Silva and Rodrigues (2006) and Kurup et al. (2006). The process is characterized by a 2-steps operation: (a) in the first step the feed is introduced while the intermediary product is recovered with the whole unit working as a fixed bed; (b) during the second step the feed stopped, the unit works as a standard SMB and the less and more retained products are collected.

6 Conclusions

Different applications of the SMB concept here considered as "old" and "new" were presented. The example of a Sorbex® UOP unit (Parex® unit for the separation of p-xylene from its C_8 isomers), was used to better describe an "old" application of the SMB technology in the petrochemical field, modelled by a TMB plus LDF approach; the use of new optimization packages in the design/optimization of SMB units was also shown. The "new" SMB application in the pharmaceutical area was illustrated with a chiral resolution; a comparison between standard SMB and non-conventional operating mode Varicol®, both modelled by the SMB model was presented.

"Old" applications are characterized by high values of productivity in large units with high number of columns, while the "new" applications show low productivities and much lower scale. There is room to improve "new" applications mainly in the development of new adsorbents with higher capacity. Interesting to note is that column aspect ratio diameter/length remain the same in both applications. New non-conventional techniques and new design/optimization methodologies applied to both "old" and "new" applications can lead to more efficient units contributing to the relevance of SMB in the area of separation science and technology.

7 Nomenclature

C_b	bulk fluid phase concentration ($\mathrm{mol \cdot m^{-3}}$)
$\langle C_p \rangle$	pores particle average concentration ($\mathrm{mol{\cdot}m^{-3}}$)
C^{Eluent}/ $\mathrm{C}^{\mathrm{Desorbent}}$	eluent/desorbent inlet concentration ($\mathrm{mol{\cdot}m^{-3}}$)

C^F	feed concentration (mol·m^{-3})
D_b	axial dispersion coefficient (m^2·s^{-1})
D_c	Column diameter (m)
K	Langmuir adsorption equilibrium constant (m^3·kg^{-1})
K^*	Linear adsorption equilibrium constant (Henry constant)
k_{LDF}	LDF mass transfer coefficient (s^{-1})
k_p	number of intraparticle mass transfer units
L_c	column axial length (m)
L_j	zone axial length (m)
NC	number of species
N_c	number of columns
n_j	number of columns per zone
PUX	purity in the extract current (%)
PUR	purity in the raffinate current (%)
Pe	Peclet number
PR	unit productivity $(\mathrm{g}\cdot(\mathrm{s\,m}\cdot{}^{3}{}_{\mathrm{adsorbent}})^{-1})$
Q	fluid/solid flowrate (m^3·s^{-1})
q^*	equilibrium solid retained concentration $(\mathrm{mol}\cdot\mathrm{m}^{-3}{}_{\mathrm{adsorbent}})$
q	adsorbed concentration $(\mathrm{mol}\cdot\mathrm{m}^{-3}{}_{\mathrm{adsorbent}})$
$\langle q\rangle$	average adsorbent phase concentration $(\mathrm{mol\,m}^{-3}{}_{\mathrm{adsorbent}})$
q_{mi}	maximum adsorbed phase concentration $(\mathrm{kg}\cdot\mathrm{kg}^{-1}{}_{\mathrm{adsorbent}})$
REX	recovery in the extract (%)
RER	recovery in the raffinate (%)
R_p	particle radius (m)
t	time variable (s)
t_j	bulk fluid space time (s)
t_s	switch time (s)
u_j	interstitial fluid velocity in a TMB/SMB zone $(\mathrm{m}\cdot\mathrm{s}^{-1})$
u_s	solid interstitial counter-current velocity $(\mathrm{m}\cdot\mathrm{s}^{-1})$
x	dimensionless axial coordinate
z	axial coordinate (m)

Greek letters

γ	ration between fluid and solid interstitial velocities
ε_b	bed porosity
ε_p	particle porosity
ρ_p	apparent solid density $(\mathrm{kg}\cdot\mathrm{m}^{-3})$
ρ_f	fluid (liquid) density $(\mathrm{kg}\cdot\mathrm{m}^{-3})$
θ	dimensionless time coordinate

Indexes

*	in the SMB model
A	p-xylene *in the Parex® example*
B	m-xylene *in the Parex® example*
C	o-xylene *in the Parex® example*
D	ethylbenzene *in the Parex® example*
E	p-diethylbenzene *in the Parex® example*
A	more retained species *in the chiral separation examples*
B	less retained species *in the chiral separation examples*
b	bulk
c	column
p	particle
s	solid
i	chemical species
j	SMB/TMB zone
Eluent	eluent stream
Desorbent	desorbent stream
Feed	feed stream
Raffinate	raffinate stream
Extract	extract stream

Abbreviations

AE,	Algebraic equations
CSS,	Cyclic Steady State
DAE,	Differential-Algebraic Equations
LDF,	Linear Driving Force
OCFEM,	Orthogonal Collocation in Finite Elements Method
ODE,	Ordinary Differential Equations
PDAE,	Partial Differential Algebraic Equations
PDE,	Partial Differential Equations
SMB,	Simulated Moving Bed
TMB,	True Moving Bed
OSS,	Outlet Streams Swing
MF,	MultiFeed

Acknowledgment Pedro Sá Gomes acknowledges the financial support from FCT "Fundação para a Ciência e a Tecnologia" (Ph-D grant SFRH/BD/22103/2005), Ministry of Science and Technology of Portugal. Financial support through the project POCI/EQU/59296/2004 is gratefully acknowledged.

This work is based on the presentation: Sá Gomes, P.; M. Minceva and A.E. Rodrigues, "Modelling, Simulation and Optimization of Cyclic Separation Processes." In: *PSE Annual*

Meeting 2006, London UK (2006), http://www.psenterprise.com/events/am_2006_presentations.html.

References

Abel, S., G. Erdem, M. Mazzotti, M. Morari, and M. Morbidelli, "Optimizing Control of Simulated Moving beds-Linear isotherm," *J. Chromatogr. A*, **1033**, 229–239 (2004).

Abunasser, N., Y.-S. Kim, Y.M. Koo, and P.C. Wankat, "One-Column Chromatograph with Recycle Analogous to a Four-zone Simulated Moving Bed," *Ind. Eng. Chem. Res.*, **42**, 5268–5279 (2003).

Adam, P.R., M. Nicoud, and M. Bailly, O. Ludemann-Hombourger, U.S. Patent No 6,136,198, 2000.

Amanullah, M. and M. Mazzotti, "Optimization of a Hybrid Chromatography-Crystallization process for the Separation of Tröger's Base Enantiomers," *J. Chromatography A*, **1107**, 36–45 (2006).

Amanullah, M., S. Abel, and M. Mazzotti, "Symposium on preparative and Industrial Chromatography and Allied Techniques," Aachen, Germany, 2004.

Araújo, J.M.M., R.C.R. Rodrigues, and J.P.B. Mota, "Use of Single-Column Models for Efficient Computation of the Periodic State of a Simulated Moving Bed Process," *Ind. Eng. Chem. Res.*, **45**, 5314–5325 (2006).

Azevedo, D.C. and A.E. Rodrigues, "Design of a Simulated Moving bed in the Presence of Mass-transfer Resistances," *AIChE J.*, **45**(5), 956–966 (1999).

Bailly, M., R.M. Nicoud, A. Philippe, and O. Ludemann-Hombourger, "Method and Device for Chromatography Comprising a Concentration Step," US patent No. WO2004039468, 2004.

Abdelmoumen, S., L. Muhr, M. Bailly, and O. Ludemann-Hombourger, "The M3C Process: A New Multicolumn Chromatographic Process Integrating a Concentration Step. I-The Equilibrium Model," *Sep. Sci. Tech.*, **41**(12), 2639–2663 (2006).

Balannec, B. and G. Hotier, "From Batch Elution to Simulated Countercurrent Chromatography," G. Ganetsos, and P.E. Barker (Eds.), in *Preparative and Production Scale Chromatography*, pp. 301–357, Marcel Dekker, New York, 1993

Blehaut, J. and R.-M. Nicoud, *Analusis Mag.*, **26**, M60 (1998).

Borges da Silva, E.A. and A.E. Rodrigues, "Methodology for the Design of Chromatographic Multicomponent Separation by a Pseudo-Simulated Moving Bed," *AIChE J.*, **52**(11), 3794–3812 (2006).

Broughton, D.B. and C.G. Gerhold, "Continuous Sorption Process Employing Fixed Bed of Sorbent and Moving Inlets and outlets," U.S. Patent No 2,985,589, 1961.

Chiang, A.S.T., "Equilibrium Theory for Simulated Moving Bed Adsorption Processes," *AIChE J.*, **44**(11), 2431–2441 (1998).

Danckwerts, P.V., "Continuous Flow Systems; Distribution of Residence Times," *Chem. Eng. Sci.*, **2**, 2 (1953).

DeVault, D., "The Theory of Chromatography," *J. Am. Chem. Soc.*, **65**, 532 (1943).

Erdem, G., S. Abel, M. Morari, M. Mazzotti, and M. Morbidelli, "Automatic Control Of Simulated Moving Beds II: nonlinear isotherm," *Ind. Eng. Chem. Res.*, **43**, 3895–3907 (2004b).

Erdem, G., S. Abel, M. Morari, M. Mazzotti, M. Morbidelli, and J.H. Lee, "Automatic Control of Simulated Moving Beds," *Industry Engineering Chemical Research*, **43**, 405–421 (2004a).

Glueckauf, E., "Theory of Chromatography part 10: Formula for Diffusion into Spheres and Their Application to Chromatography," *Trans. Faraday Soc.*, **51**, 1540–1551 (1955).

Hashimoto, K., S. Adachi, Y. Shirai, and M. Morishita, "Operation and Design of Simulated Moving Bed Adsorbers" in G. Ganetsos, and P.E. Barker, *Preparative and Production Scale Chromatography*, (Eds.) pp. 273–300, Marcel Dekker, New York, 1993.

Helfferich, F. and G. Klein, *Multicomponent Chromatography*, Marcel Dekker, New York, 1970.

Helfferich, F.G., "Multicomponent Ion Exchange in Fixed Beds: Generalized Equilibrium Theory for Systems with Constant Separation Factors," *Ind. Eng. Chem. Fundamentals*, **6**(3), 362–364 (1967).

Hur, J.S. and P.C. Wankat, "New design of Simulated Moving bed (SMB) for ternary separations," *Industry Engineering Chemical Research*, **44**, 1906–1913 (2005).

Hur, J.S. and P.C. Wankat, "Two-Zone SMB/Chromatography for Center-Cut Separation from ternary Mixtures: Linear isotherm Systems," *Industry Engineering Chemical Research*, **45**, 1426–1433 (2006).

Kasat, R.B. and S.K Gupta, "Multiobjective Optimization of an Industrial Fluidized Bed Catalytic Cracking Unit (FCCU) Using Genetic Algorithm (GA) with the Jumping Genes Operator," *Comput. Chem. Eng.*, **27**, 1785–1800 (2003).

Kaspereit, M., K. Gedicke, V. Zahn, A.W. Mahoney, and A. Seidel-Morgenstern, "Shortcut Method for Evaluation and Design of a Hybrid Process for Enantioseparations," *J Chromatography A*, **1092**, 43–54 (2005).

Kawase, M., T.B. Suzuki, K. Inoue, K. Yoshimoto, and K. Hashimoto, "Increased Esterification Conversion by Application of the Simulated Moving Bed Reactor," *Chemical Engineering Science*, **51**, 2971–2976 (1996).

Kearney, M. and K.L. Hieb, U.S. Patent No 5,100,553 (1992)

Kim, J.K. and P.C. Wankat, "Designs of Simulated-Moving-Bed Cascades for Quaternary Separations," *Industry Engineering Chemical Research*, **43**, 1071–1080 (2004).

Kim, J.K., N. Abunasser, and P.C. Wankat, "Use of Two feeds in Simulated Moving Beds for Binary Separation," *Korean J. Chem. Eng.*, **22**(4), 619–627 (2005).

Kim, J.K., Y. Zang, and P.C. Wankat, "Single-Cascade Simulated Moving Bed Systems for the Separation of Ternary Mixtures," *Industry Engineering Chemical Research*, **42**, 4849–4860 (2003).

Klatt, H.-U., F. Hanish, G. Dünnebier, and S. Engell, "Model-Based Optimization and Control of Chromatographic Processes," *Comput. Chem. Eng.*, **24**, 1119–1126 (2000).

Klein, G., D. Tondeur, and T. Vermeulen, "Multicomponent Ion Exchange in Fixed Beds: General Proprieties of Equilibrium Systems," *Ind. Eng. Chem. Fundamentals*, **6**(3), 339–351 (1967).

Kloppenburg, E. and E.D. Gilles, "Automatic Control of the Simulated Moving bed Process for C8 Aromatic Separation using Asymptotically Exact input/output Linearization," *J. Process Control*, **9**, 41–50 (1999).

Kruglov, V., "Methanol Synthesis in a Simulated Countercurrent Moving Bed Adsorptive Catalytic Reactor," *Chemical Engineering Science*, **49**, 4699–4716 (1994).

Kurup, A.S., Subramani, H.J., Hidajat, K., and Ray, A.K., "Optimal Design and Operation of SMB Bioreactor for Sucrose Inversion," *Chemical Engineering Journal*, **108**, 19–33 (2005).

Kurup, A.S., K. Hidajat, and A.K. Ray, "Comparative Study of Modified Simulated Moving bed Systems at Optimal Conditions for the Separation of Ternary mixtures Under Nonideal Conditions," *Industry Engineering Chemical Research*, **45**(11), 3902–3915 (2006).

Langmuir, I., "The velocity of Reactions in Gases moving Through Heated Vessels and the Effect of Convection and Diffusion," *J. Am. Chem. Soc.*, **30**, 1742–1754 (1908).

Lim, B.G., C.B. Ching, R.B.H. Tan, and S.-C. Ng, "Recovery of (−)-Praziquantel from Racemic Mixtures by Continuous Chromatography and Crystallisation," *Chem. Eng. Sci.*, **50,** 2289–2298 (1995).

Lode, F., M. Houmard, C. Migliorini, M. Mazzotti, and M. Morbidelli, "Continous Reactive Chromatography," *Chemical Engineering Science*, **56**, 269–291 (2001).

Lorenz, H., P. Sheehan, and A. Seidel-Morgenstern, "Coupling of Simulated Moving Bed Chromatography and Fractional Crystallisation for Efficient Enantioseparation," *J. Chromatography A*, **908**, 201–214 (2001).

Ludemman-Hombouger, O., R. Nicoud, and M. Bailly, "The "Varicol" Process: a New Multicolumn Continuous Chromatographic Process," *Sep. Sci. Tech.*, **35**(12), 1829–1862 (2000).

Ma, Z. and N.-H.L. Wang, "Standing Wave analysis of SMB Chromatography: Linear Systems," *AIChE Journal*, **43**, 2488–2508 (1997).

Mazzotti, M., G. Storti, and M. Morbidelli, "Optimal Operation of Simulated Moving Bed Units for NonLinear Chromatographic Separations," *J. Chromatography A*, **769**, 3–24 (1997).

Migliorini, C., M. Mazzotti, and M. Morbidelli, "Design of Simulated Moving Bed Multicomponent Separations: Langmuir Systems," *Sep. and Pur. Tech.*, **20**, 79–96 (2000).

Minceva, M., "Separation/Isomerisation of Xylenes by Simulated Moving Bed Technology," Ph. D. Thesis, Universidade do Porto, Portugal (2004a).

Minceva, M., and A.E. Rodrigues, "Adsorption of Xylenes on Faujasite-type Zeolite: Equilibrium and Kinetics in Batch Adsorber," *Chem. Eng. Research Design*, **82**, 667–681 (2004b).

Minceva, M. and A.E. Rodrigues, "Influence of the Transfer Line Dead Volume on the Performance of an Industrial Scale Simulated Moving Bed for p-Xylene Separation," *Sep. Sci. Tech.*, **38**(7), 1463–1497 (2003).

Minceva, M. and A.E. Rodrigues, "Modeling and simulation of a Simulated Moving bed for the Separation of *p*-Xylene," *Industry Engineering Chemical Research*, **41**, 3454–3461 (2002).

Minceva, M. and A.E. Rodrigues, "Two-Level Optimization of an Existing SMB for p-xylene Separation," *Comput. Chem. Eng.*, **29**, 2215–2228 (2005).

Morari, M. and J. Lee, "Model Predictive Control: Past, Present and Future," *Computer and Chemical Engineering*, **23(**4–5), 667–682 (1999).

Morbidelli, M. and M. Mazzotti, "Advances in Simulated Moving bed Chromatography," in "*PREP, 15th International Symposium, Exhibit Workshops on Preparative/Process Chromatography Ion Exchange, Adsorption/Desorption Processes & related Separation Techniques*," Lecture 201 Washington DC, USA, (2002) pp. 53–54.

Natarajan, S. and J.H. Lee, "Repetitive Model Predictive Control applied to a Simulated moving bed Chromatography Systems," *Computer and Chemical Engineering*, **24**, 1127–1133 (2000).

Neves, S.B., "Modelling of Adsorption Fixed–Bed in Liquid-Solid Systems," M.SC. Thesis, Universidade Federal da Bahia, Brazil, 1995.

Nicolaos, A., L. Muhr, P. Gotteland, R.M. Nicoud, and M. Bailly, "Application of Equilibrium Theory to Ternary Moving bed Configurations (four+four, five+four, eight and nine zones): I. Linear case," *J. Chromatography A*, **908**(1–2), 71–86 (2001a).

Nicolaos, A., L. Muhr, P. Gotteland, R.M. Nicoud, and M. Bailly, "Application of the Equilibrium Theory to Ternary Moving bed Configurations (4+4, 5+4, 8 and 9 zones): II. Langmuir case," *J. Chromatography A*, **908**(1–2), 87–109 (2001b).

Nicoud, R.M., "The Separation of Optical Isomers By Simulated Moving Bed Chromatography," *Pharm. Tech Europe*, **11**(3), 36 (1999a).

Nicoud, R.M., "The Separation of Optical Isomers by Simulated Moving Bed Chromatography," *Pharm. Tech Europe*, **11**(4), 28 (1999b).

Pais, L.S. and A.E. Rodrigues, "Design of Simulated Moving Bed and Varicol Processes for Preparative separations with a Low Number of Columns," *J. Chromatogr. A*, **1006**, 33–44 (2003).

Paredes, G., H.-K. Rhee, and M. Mazzotti, "Design of Simulated-Moving-Bed Chromatography with Enriched Extract Operation (EE-SMB): Langmuir Isotherms," *Ind. Eng. Chem. Res.*, **45**(18), 6289–6301 (2006).

Pavone, D. and G. Hotier, "System Approach Modelling Applied to the Eluxyl Process," *Revue IFP*, **55**, 437 (2000).

Rhee, H.-K., R. Aris, and N.R. Amundson, "On the Theory of Multicomponent Chromatography," *Phil. Trans. Roy. Soc. London A*, **296**, 419 (1970).

Rodrigues, A.E. and L.S. Pais, "Design of SMB Chiral Separations Units Using Concept of Separation Volume," *Sep. Sci. and Tech.*, **39**, 245–270 (2004).

Sá Gomes P., C.P. Leão, and A.E. Rodrigues, "Simulation of True Moving Bed Adsorptive Reactor: Detailed Particle Model and Linear Driving Force Approximations," Accepted in *Chem. Eng. Sci.* (2006).

Sá Gomes P., M. Minceva, L.S. Pais, and A.E. Rodrigues, "Advances in SMB chromatographic separations," *Chiral Separation Techniques*, in G. Subramanian (Ed.), Wiley–VCH, 2006.

Sá Gomes, P. and A.E. Rodrigues, "Outlet Streams Swing (OSS) and MultiFeed (MF) Operation of Simulated Moving Beds," Accepted in *Sep. Sci. and Tech.* (2006).

Santacesaria, E., M. Morbidelli, P. Danise, M. Mercenari, and S. Carra, "Separation of xylenes on Y zeolite. Part1. Determination of the Adsorption Equilibrium Parameters, Selectivities and Mass Transfer Coefficients Through Finite Batch Experiments," *Ind. and Eng. Chem. Proc. Des. Dev.*, **21**, 440–446 (1982).

Schramm, H., S. Gruner, A. Kienle, and E.D. Gilles, in "*Proceedings of European Control Conference 2001*," pp. 2528–2533, Porto, Portugal, (2001).

Schramm, H., M. Kaspereit, A. Kienle, and A. Seidel-Morgenstern, "Improving Simulated Moving Bed Processes by Cyclic modulation of the Feed Concentration," *Chem. Eng. Tech.*, **25**(12), 1151–1155 (2002).

Schramm, H., M. Kaspereit, A. Kienle, and A. Seidel-Morgenstern, "Simulated Moving Bed Process with a Cyclic Modulation of the Feed Concentration," *J. Chromatography A*, **1006**, 77–86 (2003).

Sherman, J.D., "Ion Exchange Separations With Molecular Sieve Zeolites," in *Zeolites: Science and Technology* F. Ribeiro, A Rodrigues, L Rollmann, and C. Naccache (Eds.) pp. 583–622, Martinus Nijhoff Pub., The Hague, 1984.

Silva, V.M.T.M. and A.E. Rodrigues, "Novel process for Diethylacetal Synthesis," *AIChE. J*, **51**, 2752 (2005).

Silva, V.M.T.M. and A.E. Rodrigues, 2004 and 2005. "Processo Industrial de Produção de Acetais num Reactor Adsorptivo de Leito Móvel Simulado," Patents PT103123 2004, and "Industrial Process For Acetals Production in a Simulated Moving Bed Reactor" WO/2005/113476.

Storti, G., M. Masi, S. Carrá, and M. Morbidelli, "Optimal Design of Multicomponent Counter-current Adsorption Separation Processes Involving Non-Linear Equilibria," *Chem. Eng. Sci.*, **44**, 1329–1345 (1989).

Storti, G., M. Mazzotti, M. Morbidelli, and S. Carrá, "Robust Design of Binary Counter-Current Adsorption Separation Processes," *AIChE J.*, **39**, 471–492 (1993).

Strube, J., G. Ströhlein, and M. Shulte, "Symposium on preparative and Industrial Chromatography and Allied Techniques," Aachen, Germany, 2004.

Tondeur, T. and G. Klein, "Constant-Separation-Factor Equilibrium," *Ind. Eng. Chem. Fundamentals*, **6**(3), 351–361 (1967).

Wang, C., K.U. Klatt, G. Dünnebier, and F. Hanisch, "Neural Network-Based identification of SMB Chromatographic Processes," *Control Eng. Pract.*, **11**(8), 949–970 (2003).

Wankat, P.C., "Simulated Moving Bed Cascades for Ternary Separations," *Industry Engineering Chemical Research*, **40**, 6185–6193 (2001).

Zhang, Z., M. Mazzotti, and M. Morbidelli, "PowerFeed Operation of Simulated Moving bed Units: Changing the Flowrates During the Switching Interval," *J. Chromatography A*, **1006**(1–2), 87–99 (2003).